CHEMISTRY OF MATERIALS

Article

pubs.acs.org/cm

Rapid and Reversible Tuning of Structural Color of a Hydrogel over the Entire Visible Spectrum by Mechanical Stimulation

Md. Anamul Haque,[†] Takayuki Kurokawa,[‡,§] Gen Kamita,[†] Youfeng Yue,[†] and Jian Ping Gong*[,‡]

[†]Division of Biological Sciences, Graduate School of Science, and [‡]Faculty of Advanced Life Science, Hokkaido University, Sapporo 060-0810, Japan

[§]Creative Research Institution, Hokkaido University, Sapporo 001-0021, Japan

Supporting Information

ABSTRACT: In this work, we report a rubberlike elastic hydrogel containing microdomains of bilayers periodically stacked into the polymer network that satisfy the Bragg's law of diffraction. The rubberlike elastic hydrogel has been synthesized by applying double network principle into a viscoelastic hydrogel containing single-domain macroscopic lamellar bilayer. The hydrogel is able to tune the magnificent structural color reversibly over the entire wavelength range of visible spectrum as fast as the uniaxial tensile stretching and compressive deformation are applied and released. Owing to the strength, softness, and rubberlike elastic deformability, the tunable hydrogel can be used extensively to design a new class of soft tactile sensor as an advanced stress sensor that is able to detect a local deformation of a complicated force field.

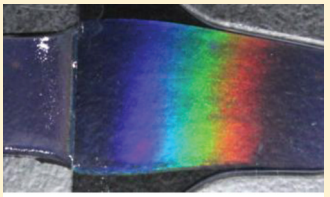

KEYWORDS: *double network, swelling, mechanical strength, tunable structural color, stress sensor*

INTRODUCTION

Recently, photonic hydrogels have attracted extensive attention in the field of sensors because of their unique optical properties arising from their periodically ordered structure.[1−18] Most of the studies, so far, are limited to the color tuning either by chemical or physical stimuli such as temperature,[8−15] pH,[15,16] solvent exchange,[17,18] etc. However, these photonic materials remain poorly applicable for devices that possess a complicated force field. Reasonably, a soft material, such as a mechanical sensor, that can detect the local stress/strain of the force field is highly demanded. So far, some attempts have been made for developing such mechanoresponsive color tuning materials based on isotropic colloidal crystal array such as photonic gel,[19] photonic crystal,[20] and inverse opal sheet.[21] However, the color of the former two materials can be tuned only by compression in the observation direction that limits its applications, whereas the latter is irreversible. Although a photonic rubber based on isotropic colloidal crystal has been developed,[22] the reversible color tuning is feasible to a small wavelength range of 30 nm in response to a maximum tensile strain of 20%. All the efforts remain out of reach for finding a novel soft material that is able to tune the color over the entire visible spectrum reversibly in a quick response with the mechanical stimuli such as uniaxial tensile stretching−releasing and compression.

Recently, we developed an anisotropic photonic hydrogel (PDGI/PAAm) in which periodically ordered single-domain lamellar bilayers of a self-assembled polymeric surfactant (dodecyl glyceryl itaconate: DGI) are entrapped inside a polymer network of polyacrylamide (PAAm). Bragg's reflection of visible light on the periodic lamellar plane caused the gel to exhibit excellent structural color and the color could be tuned by the compressive deformation.[23] However, once the gel is compressed and/or stretched, a long time (5−30 min) is required to regain its original color and dimensions that limits its applicability. The slow recovery of the color and dimensions attribute to the slow hydrophobic association of PDGI (polymerized DGI) into a well-packed bilayer.[24]

In this work, we synthesized a rubberlike elastic hydrogel material that exhibits rapid and reversible color tuning under mechanical stimuli, by forming a microdomain bialyer structure from the macrodomain bilayer of the PDGI/PAAm hydrogel. Applying the double network principle,[25] we have introduced a second PAAm network into the existing first PAAm network layers of the PDGI/PAAm hydrogel to obtain a so-called PDGI/PAAm^2 hydrogel (Figure 1a). The PDGI/PAAm^2 hydrogel diffracts light depending on the periodic distance of bilayers and shows almost purely reversible elastic behavior on mechanical deformation as like as an elastic rubber. The hydrogel, which is initially almost transparent and satisfies the Bragg's law to diffract the light in far red wavelength band, exhibits magnificent visible color at a small deformed state. This color can successfully be tuned reversibly over the entire wavelength region of visible light very quickly with the uniaxial tensile stretching and releasing of the stress. This color tuning phenomena is further observed by applying compressive deformation along the observation direction as well as perpendicular to the observation direction. The gel with an initial color of blue can also be tuned reversibly from blue to red by compressing the gel from side, i.e., perpendicular to the observation direction. The strength, softness, and rubberlike

Received: July 23, 2011
Revised: October 25, 2011
Published: November 11, 2011

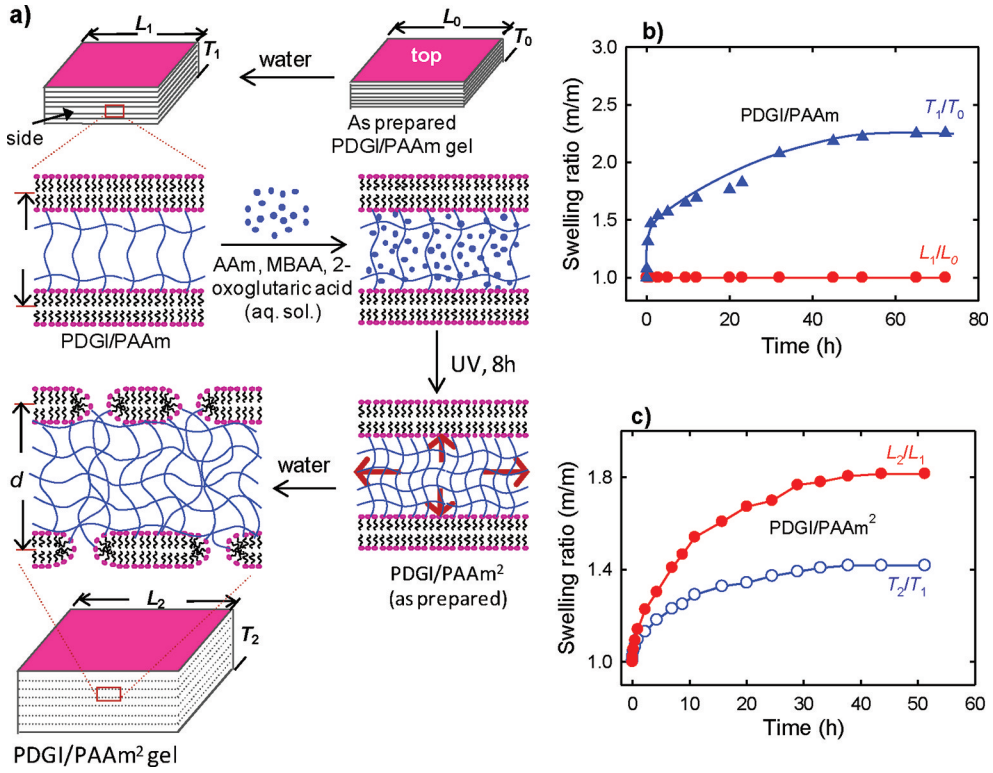

Figure 1. (a) Schematic representation for the formation of microdomain bilayer structure of PDGI/PAAm^2 gel by introducing a 2nd PAAm network into the existing PAAm network of the PDGI/PAAm gel. (b) Swelling ratio of the parent PDGI/PAAm gel increases with time along the thickness axis (perpendicular to the bilayers, T_1/T_0), while no swelling at all along the length axis (parallel to the bilayers, L_1/L_0). (c) Swelling ratio of PDGI/PAAm^2 gel along both the thickness axis (perpendicular to the bilayers, T_2/T_1) and length axis (parallel to the bilayers, L_2/L_1) increase with time but the former one is larger than the latter one. This indicates that the anisotropic swelling, though it becomes weaker, still exists, which is in the reverse of the anisotropic swelling of PDGI/PAAm gel.

elastic deformability of the tunable gel might allow its potential applicability to design a new class of soft tactile sensor. Such a sensor might be applied as an advanced stress sensor in many devices to detect external stress−strain.

EXPERIMENTAL SECTION

Gel Preparation. The parent PDGI/PAAm gel with macroscopic unidomain bilayer structure was prepared by simultaneous free radical polymerization from aqueous solution of 0.10−0.17 M dodecylglyceryl itaconate [DGI; n-$C_{12}H_{25}OCOCH_2C(=CH_2)COOCH_2CH(OH)$-$CH_2OH$], 0.025 mol % sodium dodecyl sulfate (SDS) of DGI, 2 M acrylamide (AAm), 2 mM *N,N*′-methylenebis (acrylamide) (MBAA) as a cross-linker of AAm, and 2 mM Irgacure as an initiator. The detailed procedures was described in our previous paper.[23] Briefly, the precursor solution was prepared at 55 °C for about 4 h in water bath until the equilibrium formation of stable microdomain lamellar bilayers of self-assembled DGI. Prior to the polymerization, bilayer microdomains were aligned in one direction in the macroscopic or cm-scale by applying a shear flow to the precursor solution. For this purpose, a plate-like polymerization cell (10 × 1 × 0.1 cm^3) was prepared by sandwiching silicone rubber between two glass plates. Then the precursor solution was injected into the reaction cell with a high flow speed of about 5 cm^{-1}, which created a strong shear rate of about 200 s^{-1}. Because of the strong shear flow between two parallel glass plates, thousands of bilayers (cm-scaled) were aligned in one direction parallel to the substrate surfaces. After polymerization, bilayers were stacked periodically and entrapped in the PAAm matrix to give a mechanically strong hydrogel after attaining equilibrium swelling in water. A temperature of 50−55 °C was maintained during injection and polymerization process to prevent DGI-lamellar phase separation. The parent PAAm gel was prepared similarly in the absence of DGI and SDS. The second PAAm network was introduced into the PDGI/PAAm gel and PAAm gel simply by immersing the gels into the second monomer solution containing 2 M AAm, 2 mM MBAA, and 2 mM 2-oxoglutaric acid for 7 days to ensure the equilibrium. The second network of PAAm was subsequently formed by performing 8 h UV polymerization at room temperature. The synthesized PDGI/PAAm^2 gel was then immersed in water again to attain the equilibrium swelling. Three different PDGI/PAAm^2 gels (transparent, green, and blue) were prepared from three different parent PDGI/PAAm gels by applying the identical condition for the second PAAm network formation. The concentration of DGI at preparation, wavelength at maximum of the reflection spectra (λ_{max}) of the parent PDGI/PAAm gels and the λ_{max} of the respective PDGI/PAAm^2 gels obtained by second PAAm network formation are shown in Table 1.

Table 1. Concentration of DGI at Preparation, λ_{max} of the Parent PDGI/PAAm Gels and That of the Respective PDGI/PAAm^2 Gels Obtained by 2nd PAAm Network Formation

[DGI] (mol L^{-1})	PDGI/PAAm λ_{max} (nm)	PDGI/PAAm^2 λ_{max} (nm)
0.10	597	717
0.13	461	538
0.17	383	446

Swelling Ratio Measurement. The anisotropic swelling behaviors of the hydrogel were characterized by the size ratios during/after swelling to that of the as-prepared state in directions parallel to the bilayers (length ratio, L/L_0) and perpendicular to the bilayers (thickness ratio, T/T_0). Here, we denoted the length and thickness of the parent PDGI/PAAm hydrogel at the as-prepared state as L_0 and T_0, at swelling time t as $L_1(t)$ and $T_1(t)$, and at equilibrium state as L_1 and T_1, respectively. Furthermore, we denoted the length and

dx.doi.org/10.1021/cm2021142 | *Chem. Mater.* 2011, 23, 5200−5207

thickness of the PDGI/PAAm^2 hydrogel at swelling time t as $L_2(t)$ and $T_2(t)$, and at equilibrium state as L_2 and T_2, respectively. As has been clarified in our previous paper, there was no any in-plane anisotropy of the bilayer and the size change in length and width of the sample were identical,[23] so we only discussed the swelling ratio in length in this work. The length of the gel at different swollen state was measured by a slide calipers and the thickness was measured by a tensile-compressive test machine (Tensilon RTC-1310A, Orientec Co.). To measure the thickness, we calibrated the distance between load cell and the lower plate of the tensilon to zero when the normal load started to be detected. The sample was then put into the lower plate and the load cell was approached to the sample until a load was detected. This distance between the load cell and the lower plate of tensilon gives the accurate thickness, whereas the thickness of soft gel was difficult to measure accurately by any other scales.

Transmission Electron Microscope. The hydrogel was cut into small pieces (2 mm × 2 mm × 1.2 mm) and then stained with osmium tetraoxide (OsO_4) for 5 days. After staining, the gel was immersed in water to attain equilibrium swelling state. The small pieces of gel were placed in a mold with specific shape and a hardening resin was added to the mold in such a way that the samples keep its position in the middle of the resin. The gel samples that embed into the resin were stored in an oven for 48 h to obtain the dry gel sample embedded into the hard resin. The embedded gel sample was fixed into the slice cutting machine (Ultracut; Leica EM UC6) and the resin was removed carefully from the surroundings of the gel sample. When all the resin was removed, the gel sample was appeared and only the cross-section of the gel comes to front. Finally, the cross-section of the gel with a slice thickness of 200−500 nm was cut by a glass knife and placed on the grid to observe by transmission electron microscope (Hitachi H-7650).

Tensile Test and Hysteresis. Tensile stress−strain properties of the gel samples, which were cut into dumbbell shape standardized size by the gel cutter (JIS-K6251−7), were analyzed with a commercial test machine (Tensilon RTC-1310A, Orientec Co.). Hysteresis was observed by performing the tensile loading followed by unloading in which the sample was initially stretched to a predefined strain and immediately unloading to zero strain at a fixed strain increasing/decreasing velocity. The consecutive second hysteresis cycle was performed immediately after the first cycle with identical experimental conditions.

Reflection Spectrum. A Xe lamp was used for light source to obtain the reflection spectrum. Variable angle reflection measurement optics (Hamamatsu Photonics KK, C10027A10687) were used for radiating white light on the gel and detecting the reflected light. A photonic multichannel analyzer (Hamamatsu Photonics KK, C10027) was used for analyzing the detected signal. The entire reflection spectrum was obtained by keeping both the incident (Bragg's angle) and reflection angles at 60°, and the wavelength at maximum, λ_{max}, was obtained from the reflection spectrum. The distance between two lamellar layers, d, was determined using the Bragg's law of diffraction, $2nd\sin\theta = \lambda$, where $n = 1.33$ (refractive index of water), θ is the Bragg angle or incident angle, and λ is the wavelength at maximum of the reflection spectrum.[23] The reflection spectra of the gel at different tensile strains were measured by fixing the gel sample strongly at the jaws of slide caliper and the strain was achieved from the scale of slide caliper. The reflection spectra of the gel at different compressive strains was measured by fixing the gel sample between two glass plates and the predetermined strain was achieved by placing some plastic thin film of desired thickness between the glass plates with gel. To observe the mechanical response with the rapid and repeatable tuning of the gel, we performed the reflection spectra of the gels at two strain states (0 and 3). At first the spectrum was taken at normal state, i.e., at a strain of 0. The gel was stretched up to a strain of 3, then we waited until 15 s from the first spectral measurement and then another spectrum was taken. Afterward, the gel was immediately destretched to a strain of 0 and the spectrum was measured after 15 s from the last measurement. In this way, we always maintained a time interval of 15 s between two consecutive spectral measurements and either stretching or destretching was performed in between two spectral measurements. On the whole, we completed a cycle of stretching and destretching including the spectral measurements by 30 s. For PDGI/PAAm^2 gel, this cycle was repeated for several times by spending 30 s in total for every cycle. In contrast, as the PDGI/PAAm gel did not return to the initial strain within 15 s after destretching, the spectra were taken at different time intervals until the complete recovery of the strain. It is worth noting here that we measured the physical properties, such as tensile test, reflection spectra, of the gel in air within 1 min. During such a short time, the gel has negligible evaporation.

Measurement of Response Time or Recovery Time. The dumbbell-shaped gel was fixed in two arms of a commercial test machine (Tensilon; RTC-1310A, Orientec Co.) and, stretching and destretching were performed by the machine. At first the gel was stretched at a velocity of 200 mm/min up to a strain of 4 and immediately destretched from the strain 4 to 0 at identical velocity. The machine automatically measured the experimental strain with time for both stretching and destretching. The strain experienced by the sample during stretching was identical with the experimental strain. But unlike stretching, the strain in the sample during destretching depended on the velocity and the strain recovery of the gel sample. During destretching with a velocity of 200 mm/min, if the strain in gel did not recover completely following the destretching, a residual strain in the sample was observed at low strain region. We measured the residual strain of the sample manually from the machine at different time intervals until the complete strain recovery.

■ RESULTS AND DISCUSSION

The bilayer structure of the PDGI/PAAm gel is retained in the presence of a second monomer solution containing AAm, MBAA and 2-oxoglutaric acid (Figure 1a). After polymerization, the second PAAm network forms interpenetrating network structure with the first PAAm network and the internal osmotic stress of the densely packed PAAm network of the PDGI/PAAm^2 gel become high when immerged in water. As a result, the macroscopic continuous bilayer domains are destroyed into discontinuous microdomains due to the swelling in water. The swelling ratio of the PDGI/PAAm gel along the thickness axis (perpendicular to PDGI bilayers: T_1/T_0) increased up to 2.2 with progress of time whereas no swelling is observed at all along the length axis (parallel to bilayers; L_1/L_0) (Figure 1b). This indicates the unidirectional swelling behavior, i.e., PAAm network in PDGI/PAAm gel can only swell freely perpendicular to the bilayers direction, which is in contrast to the single PAAm gel that shows isotropic swelling (Figure S1a). Due to the unidirectional swelling of PDGI/PAAm gel, the PAAm networks induce some internal stress parallel to the bilayers direction which is balanced by the rigid PDGI bilayers. At this stage, if the bilayers were destroyed, the PAAm networks become free to expand in parallel to the bilayers. This was exactly what we observed after introducing the second PAAm network, as shown in the following discussions.

After developing the second PAAm network, PDGI/PAAm^2 gel shows further swelling, when immersed in water, along the directions both parallel to the bilayers (L_2/L_1) and perpendicular to the bilayers (T_2/T_1) (Figure 1c). The increase in swelling ratio of the gel in both directions is attributed to the high internal osmotic stress of the PAAm^2 networks. However, the swelling parallel to the bilayers ($L_2/L_1 \approx 1.8$) is larger than that perpendicular to the bilayers ($T_2/T_1 \sim 1.4$) which is clearly different from the swelling of PDGI/PAAm gel (Figure 1b). Therefore, the swelling of the PDGI/PAAm^2 gel is weakly anisotropic. Since PAAm^2 gel also shows purely isotropic swelling and the swelling ratio is close to 1.4 (see Figure S1b in the Supporting Information), T_2/T_1 for PDGI/PAAm^2 gel is in

consistent with the swelling of second PAAm networks. In contrast, L_2/L_1 is larger than the swelling ratio (~1.4) due to pure second PAAm networks. This might be happened because of the pre-existed internal stress in the PAAm network of parent PDGI/PAAm gel as a result of the unidirectional swelling as mentioned earlier. Once the PAAm networks of PDGI/PAAm^2 gel become highly dense, reasonably, it exerts internal osmotic stress higher than the bilayer interaction. As a result, macroscopic bilayer domains are destroyed into microscopic ones, even with the change in bilayer packing. In addition, we assume that the change in bilayer packing also plays the role to increase the swelling ratio along the length axis because of the repulsive force between the bialyer microdomains. The detail swelling kinetics of the PDGI/PAAm and PDGI/PAAm^2 gels are underway and we will report some interesting results as an independent paper soon. The formation of bilayer microdomains from macroscopic bilayer is confirmed by the transmission electron microscope (TEM) images (Figure 2). The TEM image of PDGI/PAAm gel shows

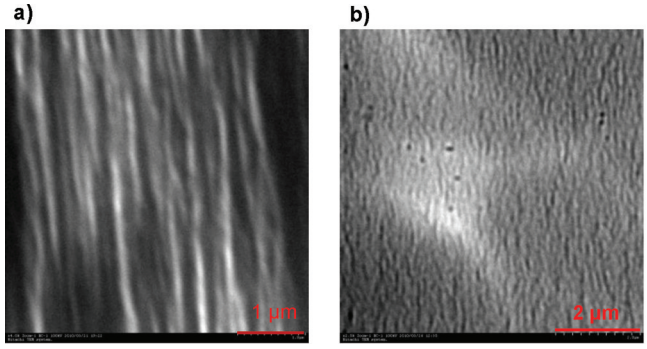

Figure 2. Transmission electron microscope images (TEM) of the PDGI/PAAm (a) and PDGI/PAAm^2 (b) gel show the long-range patterns of bilayers, i.e., macroscopic unidomain bilayers and short-range patterns of bilayers, i.e., microdomain of bilayers, respectively.

long-range patterns or macro-domains of bilayer (Figure 2a), whereas that for PDGI/PAAm^2 gel shows only short-range patterns or microdomains of bilayer (Figure 2b). One can notice that the slight distortion of bilayer structure and the deviation of average interplane distance of the bilayers, *d*, in TEM images. This might be due to the shrinkage of the gel to more than half of the initial thickness during the drying of the gel sample (shrinking of soft PAAm networks) and the distortion induced during the slicing of the cross-section of the gel to obtain a slice with a thickness of 200−500 nm for the TEM observation. However, the TEM images justify the existence of two different types of structural patterns.

Concomitant with the formation of PDGI bilayer microdomains by subsequent swelling, the PDGI/PAAm^2 gel shows a rubberlike elastic behavior with fracture stress and strain of 340 kPa and 11, respectively (Figure 3a). This indicates the high strength of the material that can sustain high load in the order of several hundreds kPa. The stress−strain curve of the PDGI/PAAm^2 gel does not show any yielding as like as PAAm and PAAm^2 gel. The slight curvature appeared at low strain in the stress−strain curve of PDGI/PAAm^2 gel, which is also observed in PAAm^2 gel, is a common feature of chemically cross-linked gel.[26] In sharp contrast, a distinct yielding is observed for the parent PDGI/PAAm gel. The yielding reveals the bilayer structure change, i.e., dissociation of hydrophobically aggregated PDGI bilayers.[24] No yielding for the PDGI/PAAm^2 gel indicates the absence of significant change of bilayer structure on elongation. The overall elastic modulus of the PDGI/PAAm^2 gel parallel to the bilayers (~6 kPa) is found on the order of PAAm^2 gel (~5 kPa) which is much smaller than that of the parent PDGI/PAAm gel (~100 kPa).[23] The absence of yielding, similar level of elastic modulus, and overlapping of stress−strain curve at low strain with PAAm^2 gel further indicate the formation of microdomains of bilayer in PDGI/PAAm^2 gel.

We assume that during tensile loading, most of the deformation is localized at the junctions of bilayer microdomains as well as in the PAAm^2 network and only the elastic chain deformation is experienced (Figure 3b), which has less contribution to the overall elastic modulus of the PDGI/PAAm^2 gel parallel to the bilayers in comparison to that of the parent PDGI/PAAm gel. Upon unloading, the elastic chain is regained to its original state immediately following the unloading exhibiting negligible hysteresis (Figure 3c), whereas PAAm^2 gel does not exhibit any hysteresis (Figure 3c, inset). The loading−unloading cycle is further repeatable within the experimental time. This further indicates the negligible dissociation of bilayer microdomains of PDGI/PAAm^2 gel during tensile elongation at low strain (<4). Consequently, the PDGI/PAAm^2 gel is recovered quickly driven by the elastic and/or entropic restoring force of the PAAm chain. On the contrary, PDGI/PAAm gel exhibits large hysteresis (Figure 3d), indicating an energy dissipation mechanism by dissociation of bilayers, and it takes several minutes to recover because of the slow hydrophobic association of DGI.

The bilayer microdomains of PDGI/PAAm^2 gel are aligned periodically almost in one direction along the top surface (length and width axes) of the platelike sample (see Figure S2 in the Supporting Information) as like as macroscopic bilayer of parent PDGI/PAAm gel, which meets the Bragg's law of diffraction of visible light. The PDGI/PAAm^2 gel, which is almost transparent, exhibits color at low tensile strain, and the color changes from red to blue-violet with the gradual increase in strain (see Movie-1 in the Supporting Information). This color change is reversible, i.e., the gel changes its color under an applied tensile stress/strain and then returns to its initial color and dimensions immediately following the quick release of the stress/strain. This color tuning phenomenon can be repeated for many times and the gel behaves like an elastic rubber during stretching and releasing. The photographs and the reflection spectra of the PDGI/PAAm^2 gel taken at different tensile strains are shown in images a and panel b in Figure 4, respectively. The reflection spectra show a shift in peak position from higher to lower wavelength in accordance with the blue shift of color with the gradual increase in strain. Since elongation accompanies with the decrease in gel thickness, i.e., compressive deformation perpendicular to stretching direction, the interbilayer distance, *d*, decreases with elongation (Figure 3b). As a result, lower wavelength light is reflected and consequent blue shift of color is observed.

The wavelengths at maximum of the reflection spectra taken at various tensile strains ($\lambda_{max;ten}$) shows a nonlinear decrease with the increase of tensile strain (ε_{ten}) and returns back in the similar way on releasing of strain (Figure 4c) indicating the reversibility in agreement with the reversible color change that we can directly observe in the real time movie (see Movie-1 in the Supporting Information). In addition, we have found that the relative change in thickness of the gel ($\Delta T/T_0$), i.e., the uniaxial compressive deformation along thickness axis increased

dx.doi.org/10.1021/cm2021142 | *Chem. Mater.* 2011, 23, 5200−5207

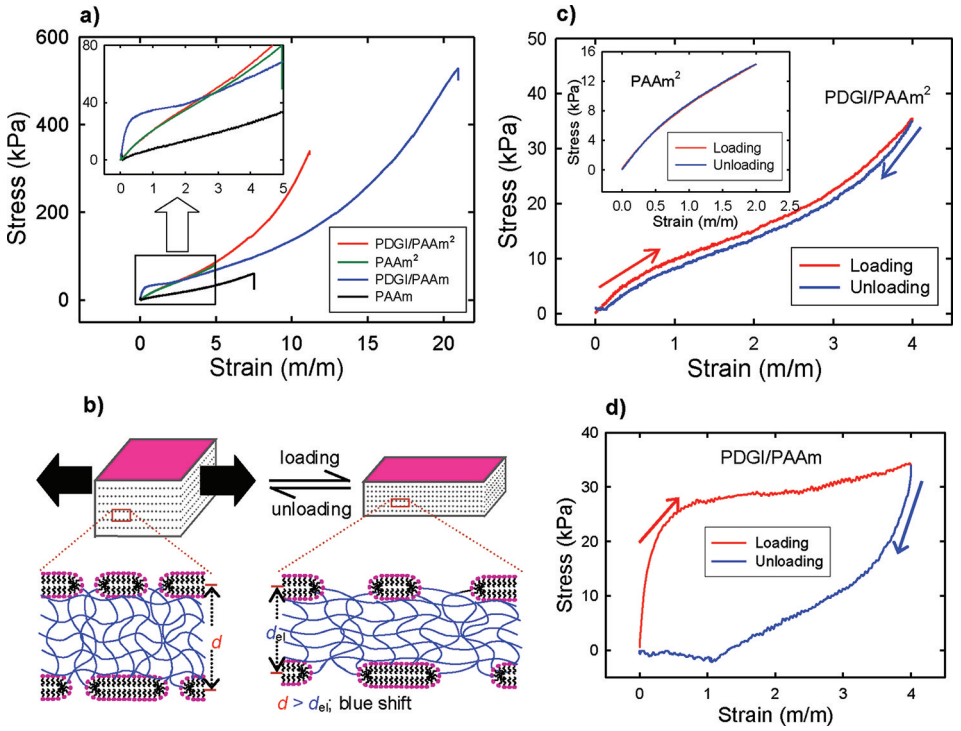

Figure 3. (a) Parent PDGI/PAAm gel shows a sharp yielding at low strain. In sharp contrast, the PDGI/PAAm^2 gel shows almost pure elastic stress−strain behavior similar to conventional chemically cross-linked gel (PAAm and PAAm^2). At low strain, the stress−strain curves of PDGI/PAAm^2 and PAAm^2 overlap with each other due to the stress concentration only in the PAAm networks. This indicates that the macroscopic continuous bilayer structure is destroyed into discontinuous domains by swelling and no further significant structure change of the bilayer domain occurs upon elongation at low strain. (b) During elongation, most of the tensile deformation is localized at the junctions of bilayer microdomains with only a fraction in the bilayers causing a decrease in interbilayer distance. (c) The negligible hysteresis for the PDGI/PAAm^2 gel almost similar to the PAAm^2 gel (inset) further indicates that there is no large change in bilayer structure during small elongation, i.e., bilayers destroyed previously. (d) During tensile loading−unloading cycles, PDGI/PAAm gel exhibits a large hysteresis as an energy dissipation mechanism because of fracture of macrodomain bilayers.

nonlinearly with the increase in tensile strain (ε_{ten}) along length axis of the gel sample (see Figure S3a in the Supporting Information). This is because compressive deformation along the width axis also occurred during uniaxial elongation along the length axis (see Figure S3b in the Supporting Information). It is found that $\lambda_{max;ten}$ decrease linearly with $\Delta T/T_0$ over the entire wavelength band of visible color (∼400−700 nm) (Figure 4c; inset). This fact can be further supported by the results that obtained by applying direct compression along the thickness axis of the gel sample which is shown later.

We further measured the response time or recovery time of the PDGI/PAAm^2 and PDGI/PAAm gels as demonstrated in Figure 5a. At first, the gel was strained up to 4 at a stretching velocity of 200 mm/min and immediately destretched to zero strain at identical velocity. Reasonably, the stretching curve is same for both the gels. For PDGI/PAAm^2 gel, the strain follows the experimental destretching with almost zero residual strain (Figure 5a; bottom). So the mechanical response of this gel during destretching is very fast (∼15 s), because the strain is completely recovered within 15 s when the gel is destretched from a strain of 4 to 0. In sharp contrast, the strain in the PDGI/PAAm gel does not completely follow the experimental destretching and shows a residual strain of ∼1.1 (Figure 5a; top). The gel then takes about 900 s to reach the initial strain ($\varepsilon \approx 0$) and consequently has poor mechanical response when destretched from a strain of 4 to 0. Concomitant with the slow mechanical response, reflection peak (λ_{max}) for the PDGI/PAAm gel shifts from higher (∼597 nm) to lower (∼396 nm) wavelength region after stretching from a strain of 0 to 3, however, after destretching, λ_{max} increases gradually with time and it takes about 900 s to return the original peak wavelength (∼597 nm) equal to that before stretching (Figure 5b; top). On the contrary, the PDGI/PAAm^2 gel takes only few seconds (∼15 s) to return the color as well as reflection peak (λ_{max}) to the original position/state (Figure 5b; bottom). Peak wavelength (λ_{max}) of the PDGI/PAAm^2 gel is about 715 nm at normal state ($\varepsilon \approx 0$) and it shifts by ∼330 nm (from ∼715 to ∼385 nm) upon stretching up to a strain of 3. With immediate destretching, λ_{max} returns to its original position (∼715 nm) by 15 s. This stretching and destretching cycle was repeated several times where a total of 30 s is required in every complete cycle and each step in one cycle either stretching or destretching requires 15 s. The color shift cycles are reproducible for many times (4 times shown here) (Figure 5b, bottom). Therefore, it can be concluded that both the deformations and color of the PDGI/PAAm^2 gel are highly reversible and respond very quickly (∼15 s), and remain stable to the extended cycles.

The PDGI/PAAm gel also appears as red at low compressive strain and the color shifts from red to blue upon gradual increase in applied compressive strain (Figure 6a, inset images, and Movie-2 in the Supporting Information). The blue shift of color is observed due to the decrease in the inter bilayer distance. Because, during compression from top of the gel, almost all the compressive deformation is localized in the PAAm layer causing a decrease in the interbilayer distance, d.[23]

dx.doi.org/10.1021/cm2021142 | Chem. Mater. 2011, 23, 5200−5207

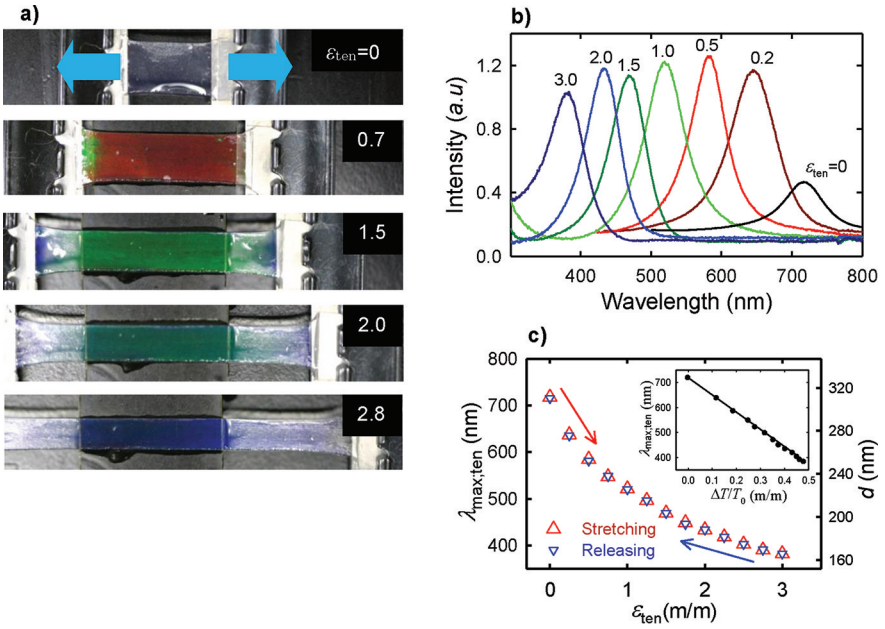

Figure 4. Reversible color tuning of the PDGI/PAAm^2 gel by tensile elongation. (a) The photographs of the gel taken at different tensile strains (ε_{ten}) show the shift of gel color from red to blue-violet with gradual increase in strain. (b) The reflection spectra (Bragg's incident angle = 60°) taken at different tensile strains (ε_{ten}) show the shift of peak position from higher wavelength (far red) to lower wavelength region (violet). The reflection spectra taken at reverse stretching are not shown to avoid overlapping. (c) The wavelength at maximum of the reflection spectrum ($\lambda_{max;ten}$) and bilayer distance, d, decreases nonlinearly with stretching, i.e., the increase in tensile strain (ε_{ten}) and follows the same way on releasing the strain (in the reverse of stretching) indicating the reversibility. $\lambda_{max;ten}$ decreases linearly with the relative change of sample thickness ($\Delta T/T_0$) perpendicular to the stretching direction at corresponding tensile strain (ε_{ten}).

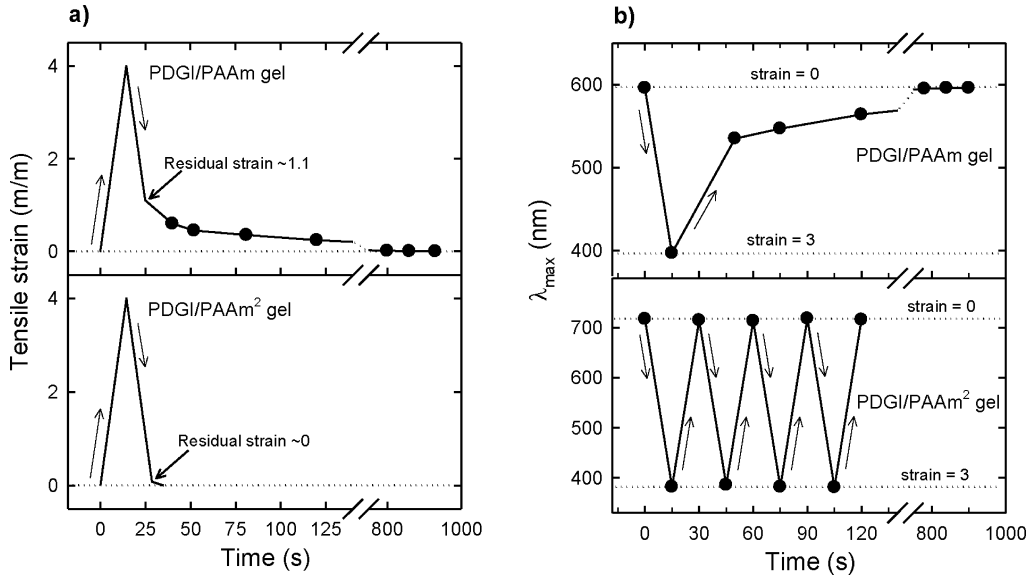

Figure 5. (a) Recovery of the strains in the PDGI/PAAm gel (top) and PDGI/PAAm^2 gel (bottom) are plotted against time. The PDGI/PAAm gel takes longer time (900 s) to recover completely the strain, whereas the PDGI/PAAm^2 returns to the original state within 15 s. (b) The shift in peak position with stretching and destretching cycles for the PDGI/PAAm gel (top) and PDGI/PAAm^2 gel (bottom) against time. For PDGI/PAAm^2 gel, every complete cycle is reproducible several times with an elapsed time of 30 s in each cycle.

The wavelengths at maximum of the reflection spectrum taken at different compressive strains ($\lambda_{max;com}$) as a function of compressive strain (ε_{com}) are also shown in Figure 6a. Concomitant with the linear behavior of $\lambda_{max;ten}$ with relative change of thickness, $\lambda_{max;com}$ also shows a linear decrease with the increase of the applied compressive strain (ε_{com}) over the entire visible spectrum (~400−700 nm). This further reveals the rapid and reversible color tuning over the entire wavelength region of visible color by compressive mechanical stimulation.

The hydrogel exhibits rainbowlike complete visible spectrum (red to violet) under a compressive strain gradient from 0 to 0.6, which might enable to detect an uneven force distribution (Figure 6b and Movie-3 in the Supporting Information). At lower compressive strain region ($\varepsilon_{com} \approx 0.2$), the interbilayer distance decrease a little which satisfy to diffract light

dx.doi.org/10.1021/cm2021142 | *Chem. Mater.* 2011, 23, 5200−5207

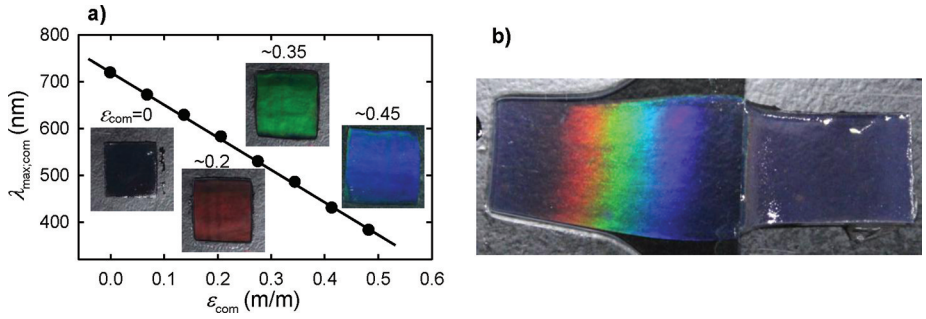

Figure 6. (a) Wavelength at maximum of the reflection spectrum taken at different applied compressive strains ($\lambda_{max;com}$) shows linear decrease with the compressive strain (ε_{com}), in agreement with the linear decrease of $\lambda_{max;ten}$ with relative change of sample thickness. The color shift of the gel from red to blue-violet is also demonstrated by the inserted images taken at different compressive strains. (b) The gel shows a complete visible spectra (rainbow) by applying a compressive strain gradient (ε_{com} = 0–0.6) on the gel with a transparent glass plate.

corresponding to the red wavelength band. With further increase in strain, the color gradually shifts to blue-violet ($\varepsilon_{com} \approx 0.45$) region because of a decrease in the corresponding interbilayer distance. At high compressive strain ($\varepsilon_{com} > 0.5$), the bilayer distance becomes too small, which diffracts light beyond the visible region and the gel become transparent in this region.

To increase the scope of applicability of this hydrogel, we successfully tuned the color of the gel by changing the compression direction. The hydrogel with an initial color of blue can also be tuned reversibly from blue to red by compressing the gel from the side, i.e., compression perpendicular to the observation direction (Figure 7a and

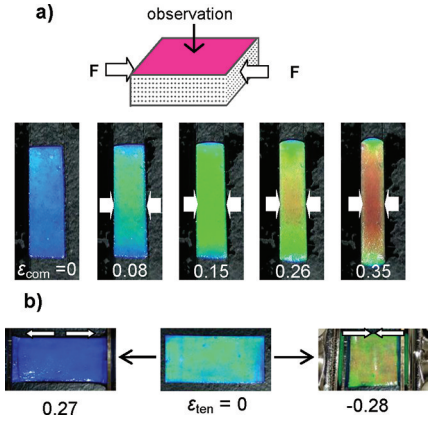

Figure 7. (a) Gel with an initial color of blue shifts the color reversibly from blue ($\varepsilon_{com;side}$ = 0) to red ($\varepsilon_{com;side}$ = 0.35) under compression from the side of the gel. (b) The gel with a color of green (tensile strain, ε_{ten} = 0) in the middle of visible spectrum region shows both blue (ε_{ten} = 0.27) and red shift (ε_{ten} = −0.28), reversibly, by tensile stretching (ε_{ten} = 0.27) and compressing along the stretching direction, i.e., negative stretching, respectively. This indicates the reversible color tuning of the gel from a middle spectral region to both way by mechanical stimulation.

Movie-4 in the Supporting Information). Due to compression from the side of the gel, the thickness as well as bilayer distance, *d*, increases resulting in a red shift of color (see Figure S4 in the Supporting Information). This color tuning phenomenon might overcome the problem associated with some force fields in which compression along the observation direction limits its applications. We also found that the hydrogel with an intermediate color of visible range (for example: green) shows both the red and blue shifts in color by linear uniaxial stretching and compressing along the stretching axis, respectively (Figure 7b and Movie-5 in the Supporting Information). When the gel with a green color is elongated, the color shifts to blue-violet because of the decrease in bilayer distance and the gel exhibits red shift in color by compressing along the elongation axis because of the increase in bilayer distance.

CONCLUSIONS

Applying the double network principle, we developed a rubberlike soft and elastic hydrogel that exhibits magnificent visible color under mechanical stimuli. The structural color of the hydrogel could successfully be tuned reversibly over the entire visible spectrum as rapidly as the tensile and/or compressive mechanical deformation is applied and released. To the best of our knowledge, such large, rapid, and reversible color tuning of a mechanically strong hydrogel by both elongation and compression have never been reported yet. Moreover, the hydrogel with a color of blue could be tuned in the reverse direction, i.e., red shift by compressing the gel from the side or perpendicular to the observation direction, which might further explore its scope in applications. The strength, softness, and rubberlike elastic deformability of the tunable gel could underpin its scope as smart sensing such as a new class of soft tactile sensor or mechanical sensor to be used under water.

ASSOCIATED CONTENT

Supporting Information

Film clips; movie legends, the swelling behavior of PAAm and PAAm^2 gel, polarizing optical microscope images of PDGI/PAAm^2 gel, relative change of thickness of gel with tensile strain, and some illustrative explanations (PDF). This material is available free of charge via the Internet at http://pubs.acs.org/.

AUTHOR INFORMATION

Corresponding Author

*Tel. & Fax: +81-11-706-2774. E-mail: gong@sci.hokudai.ac.jp.

ACKNOWLEDGMENTS

This study was supported by a Grant-in-Aid for Specially Promoted Research (18002002) from the Ministry of Education, Culture, Sports, Science and Technology of Japan.

REFERENCES

(1) Hu, Z.; Lu, X.; Gao, J.; Wang, C. *Adv. Mater.* **2000**, *12*, 1173.

(2) Cai, T.; Marquez, M.; Hu, Z. *Langmuir* **2007**, *23*, 8663.
(3) Takeoka, Y.; Watanabe, M. *Adv. Mater.* **2003**, *15*, 199.
(4) Nakayama, D.; Takeoka, Y.; Watanabe, M.; Kataoka, K. *Angrew. Chem., Int. Ed.* **2003**, *42*, 4197.
(5) Holtz, J. H.; Asher, S. A. *Nature (London)* **1997**, *389*, 829.
(6) Asher, S. A.; Alexeev, V. L.; Goponenko, A. V.; Sharma, A. C.; Lednev, I. K.; Wilcox, C. S.; Finegold, D. N. *J. Am. Chem. Soc.* **2003**, *125*, 3322.
(7) Foulger, S. H.; Jiang, P.; Lattam, A.; Smith, D. W.; Balato, J.; Dausch, D. E.; Grego, S.; Stoner, B. R. *Adv. Mater.* **2003**, *15*, 685.
(8) Hu, Z. B.; Huang, G. *Angrew. Chem., Int. Ed.* **2003**, *42*, 4799.
(9) Cai, T.; Wang, G.; Thompson, S.; Marquez, M.; Hu, Z. *Macromolecules* **2008**, *41*, 9508.
(10) Takeoka, Y.; Watanabe, M. *Langmuir* **2003**, *19*, 9104.
(11) Takeoka, Y.; Seki, T. *Langmuir* **2006**, *22*, 10223.
(12) Matsubara, K.; Watanabe, M.; Takeoka, Y. *Angew. Chem., Int. Ed.* **2007**, *46*, 1688.
(13) Debord, J. D.; Lyon, L. A. *J. Phys. Chem. B* **2000**, *104*, 6327.
(14) Asher, S. A.; Weissman, J. M.; Sunkara, H. B.; Tse, A. S. *Science* **1996**, *274*, 959.
(15) Huang, G.; Hu, Z. *Macromolecules* **2007**, *40*, 3749.
(16) Lee, Y. J.; Braun, P. V. *Adv. Mater.* **2003**, *15*, 563.
(17) Hu, Z.; Lu, X; Gao, J. *Adv. Mater.* **2001**, *13*, 1708.
(18) Zhou, B; Gao, J; Hu, Z. *Polymer* **2007**, *48*, 2874.
(19) Iwayama, Y.; Yamanaka, J.; Takiguchi, Y.; Takasaka, M.; Ito, K.; Shinohara, T.; Sawada, T.; Yonese, M. *Langmuir* **2003**, *19*, 977.
(20) Arsenault, A. C.; Clark, T. J.; Freymann, G. V.; Cademartiri, L.; Sapienza, R.; Bertolotti, J.; Vekris, E.; Wong, S.; Kitaev, V.; Manners, I.; Wang, R. Z.; John, S.; Wiersma, D.; Ozin, G. A. *Nat. Mater.* **2006**, *5*, 179.
(21) Sumioka, K.; Kayashima, H.; Tsutsui, T. *Adv. Mater.* **2002**, *14*, 1284.
(22) Fudouzi, H.; Sawada, T. *Langmuir* **2006**, *22*, 1365.
(23) Haque, M. A.; Kamita, G.; Kurokawa, T.; Tsujii, K.; Gong, J. P. *Adv. Mater.* **2010**, *22*, 5110.
(24) Haque, M. A.; Kurokawa, T.; Kamita, G.; Gong, J. P. *Macromolecules* **2011**, DOI: 10.1021/ma201653t.
(25) Gong, J. P.; Katsuyama, Y.; Kurokawa, T.; Osada, Y. *Adv. Mater.* **2003**, *15*, 1155.
(26) Ito, K. *Polym. J.* **2007**, *39*, 489.